Astron. Astrophys. 338, 576–580 (1998)

ASTRONOMY AND ASTROPHYSICS

Carbon monoxide observations of the HH 135/136 complex

K. Ogura[1], **M. Nakano**[2], **K. Sugitani**[3], **and T. Liljeström**[4,5]

[1] Kokugakuin University, Higashi, Shibuya-ku, Tokyo 150-8440, Japan (ogura@kokugakuin.ac.jp)
[2] Oita University, Oita 870-1192, Japan (mnakano@cc.oita-u.ac.jp)
[3] Institute of Natural Sciences, Nagoya-City University, Mizuho-ku, Nagoya 467-0862, Japan (sugitani@nsc.nagoya-cu.ac.jp)
[4] Metsahovi Radio Research Station, Helsinki University of Technology, Otakaari 5.A, FIN-02150 Espoo, Finland (tarja.liljestrom@hut.fi)
[5] Observatory, P.O. Box 14, FIN-00014 University of Helsinki, Finland

Received 10 March 1998 / Accepted 30 June 1998

Abstract. We report CO (J=2-1) and ^{13}CO (J=2-1) observations of the HH 135 and 136 complex, which has been mapped with the SEST radio telescope. The ^{13}CO (J=2-1) emission does not peak at the IRAS position but about 12″ away from it, probably due to a displacement of the density peak caused by radiation-driven implosion. The mass estimate of the cloud core associated with the HH complex is some 150 $M_{\odot}$. The position-velocity diagram of the CO (J=2-1) line emission reveals high velocity wings in the vicinity of the power source IRAS 11101-5829. The redshifted and blueshifted CO wing emission overlaps spatially and shows only a slight indication of bipolarity. This can be explained by a combination of a wide opening angle of the molecular outflow and the large beam size compared to its extent. In order to explain the complicated velocity structure reported for the optical outflow (Ogura & Walsh 1992), we propose a model in which the jetlike outflow from IRAS 11101-5829 is collisionally deflected by the cloud core. This view appears to be supported by the slight misalignment of HH136 knots and a possible temperature enhancement around the suspected point of impact.

Key words: ISM: jets and outflows – ISM: clouds – ISM: Herbig-Haro objects – ISM: individual objects: HH 135/136 – stars: pre-main sequence – radio lines: ISM

1. Introduction

A pair of Herbig-Haro (HH) objects HH 135/136 were discovered by Ogura & Walsh (1992, hereafter referred to as OW92) in the Carina region in a bright-rimmed cloud (No. 64 in the catalogue of Sugitani & Ogura 1994). Located at a distance of 2.7 kpc these are the most distant and intrinsically most luminous HH objects known so far. They lie close to each other and the IRAS point source 11101-5829 is located between them. All the HH knots and the IRAS source form almost a straight line. This fact as well as the morphology of some of the knots suggests opposite flow directions. Therefore HH 135 and 136 look like a usual bipolar HH pair. However, the velocity structure of the HH knots (OW92) does not support such a simple interpretation; both HH 135 and the main part of HH 136 are blueshifted and only the southwestern part of HH 136 is redshifted. In view of this complicated velocity structure, OW92 suggested that the complex may consist of two independent outflows; HH 135 is powered by IRAS 11101-5829, HH 136 by its own exciting source embedded somewhere inside it, and the southwestern part of HH 136 corresponds to the receding lobe(s) of either one or both of the two flows.

Very recently, Tamura et al. (1997) have carried out JHK polarimetric observations of HH 135/136 and concluded that IRAS 11101-5829 is the single illuminating source of the whole infrared nebula associated with the HH complex. There are some HH complexes which originate from a binary source driving two separate outflows, e.g., HH 1/2 plus HH 144+145 (Reipurth et al. 1993; Eislöffel et al. 1994) and HH 111 plus HH 121 (Gredel & Reipurth 1993). However, since IRAS 11101-5829 has, at present, no positive, but rather some negative evidence for its binarity (see Sect. 4), we adopt in the following the ordinary interpretation that the bipolarity of HH 135 and HH 136 is formed by a single outflow system. Therefore, a mechanism (or mechanisms) is needed to explain the fact that blueshifted optical emission is seen on both sides of the power source.

We have undertaken CO (J=2-1) and ^{13}CO (J=2-1) molecular line observations of this intriguing HH complex in order to study the structure and properties of the cloud core as well as to search for an associated molecular outflow. With these radio data we hoped to clarify the above velocity issue concerning the optical outflow.

2. Observations

The observations were carried out with the 15-m Swedish-ESO Submillimetre Telescope (SEST)[1] in the CO (J=2-1) and ^{13}CO (J=2-1) transitions in December 1992. The telescope and instrumentation are described by Booth et al. (1989). The front-end was an SIS mixer-receiver, and the back-end a 2000 channel

Send offprint requests to: K. Ogura

[1] SEST is operated jointly by ESO and the Swedish National Facility for Radio Astronomy, Onsala Space Observatory at Chalmers University of Technology.

acousto-optical spectrometer with a 100 MHz bandwidth and a channel separation of 43 kHz (corresponding to 0.12 km s^{-1} at 230 GHz). The half-power beam width of the antenna is 22″ at 230 GHz. The telescope pointing was checked with five-point measurements of the 86 GHz SiO maser source R Car.

The observations were made in the position-switching mode. The centre position for the mapping observations was IRAS 11101-5829 (RA_{1950} = 11^h 10^m 07^s.4; DEC_{1950} = −58° 30′ 00″). Since the optical outflow is aligned along a position angle, PA, of about 38°, the mapping was performed with a tilt angle of 38°. In CO (J=2-1) an inner area of 60″ × 60″ and an outer area of 240″ × 150″ were mapped with a grid spacing of 15″ and 30″, respectively. In ^{13}CO (J=2-1) the inner area was mapped with a 10″ grid spacing.

The standard chopper-wheel technique (Ulich & Haas 1976) is used at SEST to transform the antenna temperatures to the quantity $T_A{}^*$, which corrects for the atmospheric attenuation and ohmic losses. In order to correct for the forward spillover and scattering, we derive the quantity $T_R{}^* = (1/\eta_{fss})\, T_A{}^*$, where the forward spillover and scattering efficiency, η_{fss}, is 0.87 and has been determined by observations of the Moon. For consistency with the convention of Kutner & Ulich (1981), we present our figures in terms of $T_R{}^*$. The mean sensitivity reached in our CO (J=2-1) and ^{13}CO (J=2-1) observations was 0.13 K and 0.33 K, respectively.

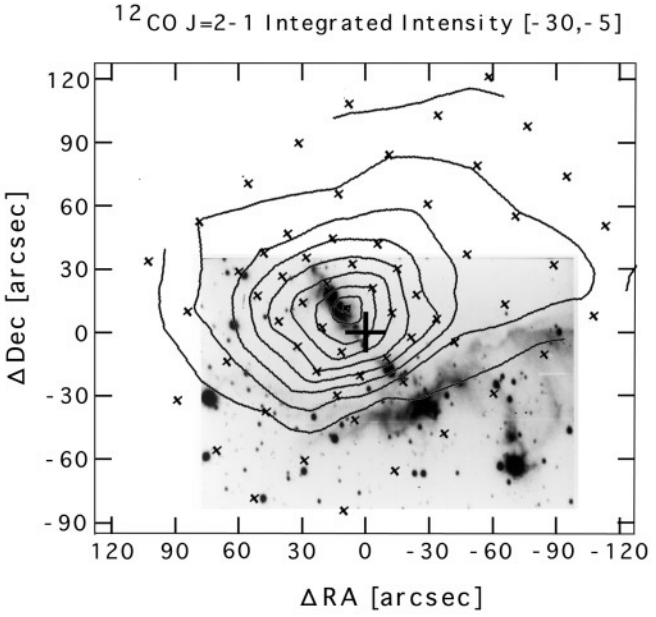

Fig. 1. Map of CO (J=2-1) line emission integrated over the velocity range −30 to −5 km s^{-1}, overlaid on the [SII] image of the HH 135/136 region. IRAS 11101-5829 is marked by a plus sign, and the observed positions are indicated by crosses. The peak contour corresponds to 135 K km s^{-1} and the contour step is 15 K km s^{-1}. Note that the molecular cloud is precisely outlined by the bright rim.

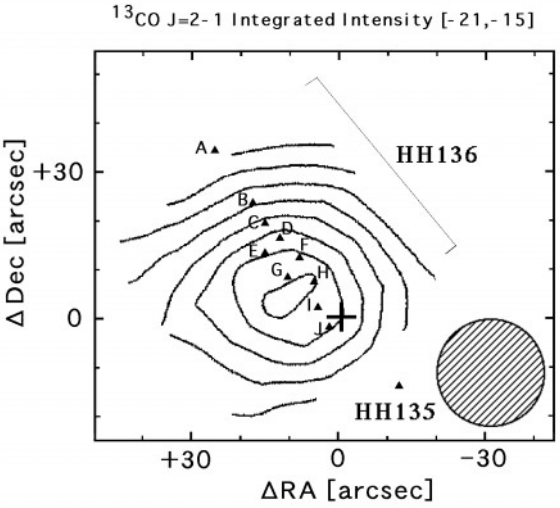

Fig. 2. Map of the ^{13}CO (J=2-1) emission in the HH 135/136 region integrated over −21 to −15 km s^{-1}. IRAS 11101-5829 and knots of the HH objects are marked by a plus sign and triangles, respectively. The peak contour corresponds to 25 K km s^{-1} and the contour interval is 1 K km s^{-1}. The FWHM beam size is shown by the hatched circle.

3. Results

Fig. 1 shows the integrated CO (J=2-1) line map overlaid on an [SII] image of the HH 135/136 region (OW92). It is seen that the molecular cloud is closely outlined by the bright HII rim in the south and southwest. Fig. 2 presents the contour map of the integrated ^{13}CO (J=2-1) line emission. In this figure IRAS 11101-5829 is marked with a plus sign and the HH knots with triangles. It is clearly seen that the ^{13}CO cloud core is displaced about 12″ toward NE from the IRAS source, i.e., further away from the bright rim. This is contrary to many other HH objects (e.g., Stapelfeldt & Scoville 1993). Probably, after the formation of IRAS 11101-5829 in the cloud core, the density peak moved along the symmetry axis of the bright rim, in accordance with the numerical simulations of radiation-driven implosions (Lefloch & Lazareff 1994). We note that HH 46/47, which is associated with the bright-rimmed cloud No. 52 of Sugitani & Ogura (1994), shows a similar displacement of the density peak of the cloud from the outflow source, i.e., towards the tail of the globule (see Fig. 2 of Olberg et al. 1992).

The mass of the cloud associated with HH 135/136 can be estimated when the column density at each grid position and the half-power size of the cloud are known. The half-power size of the integrated CO line map is 73″ × 57″, which is quite well covered by the 60″ × 60″ (0.78 pc × 0.78 pc) ^{13}CO map. Assuming LTE (i.e., $T_{ex}(^{12}CO) = T_{ex}(^{13}CO)$) and a ^{13}CO abundance ratio given by the relation $N(H_2) = (5.0 \pm 2.5) \times 10^5\ N(^{13}CO)$ (Dickman 1978; Blake et al. 1987), we calculated the column density at each grid position of the ^{13}CO map. We adopted $T_{ex}(^{13}CO)$ = 19 K (the value at the center position) over the whole cloud core. This resulted in a mass estimate of 150 $M_\odot$ for the CO cloud inside the half-power emission; however, the uncertainty in the abundance ratio, the non-uniformity of the cloud temperature, and the 50% error bar in the $N(H_2)$ relation above, cause a crude nature of our mass estimate.

Fig. 3 displays the position-velocity diagram of the CO (J=2-1) line emission along the axis of HH 135/136. It demonstrates

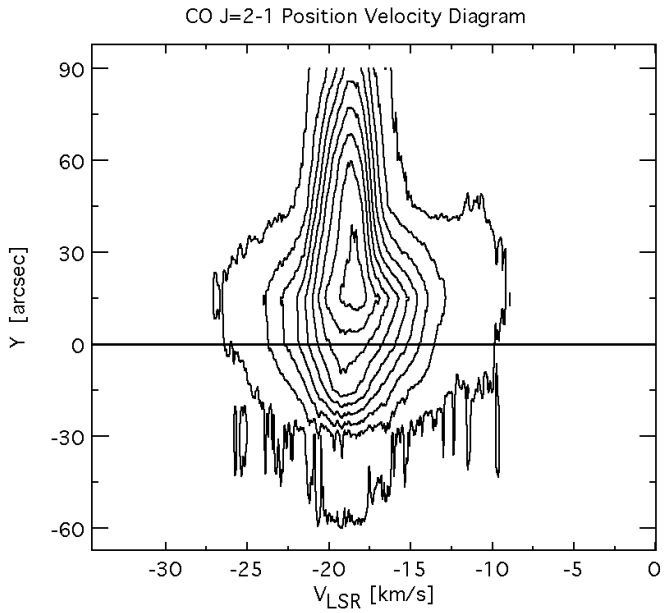

Fig. 3. Position-velocity diagram of the CO (J=2-1) line emission along the axis of HH 135/136. High velocity wing emission is evident. The contour intervals are 2 K, starting with the 2 K contour.

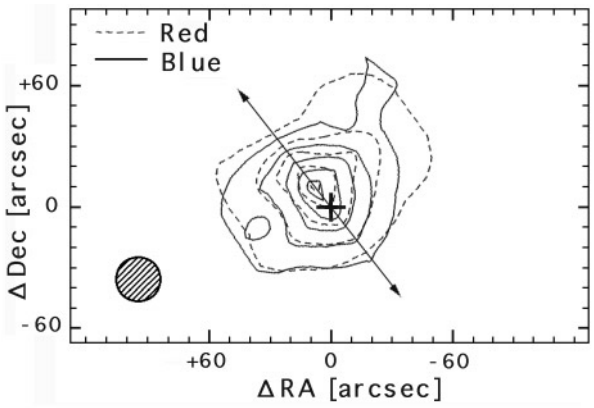

Fig. 4. Maps of CO (J=2-1) high velocity wing components. The arrow indicates the approximate orientation of the optical outflow of PA=38°. Solid and dashed contours represent the blueshifted emission ($-29 < V_{LSR} < -21$ km s^{-1}) and the redshifted emission ($-15 < V_{LSR} < -7$ km s^{-1}), respectively. The contours are separated by 3 K km s^{-1} and begin at 3 K km s^{-1}. The beam size in FWHM is shown by the hatched circle.

the presence of high velocity wing components. A line profile analysis shows that the high velocity components extend up to -15 km s^{-1} and $+15$ km s^{-1} with respect to the systemic LSR velocity of the cloud core (-19 km s^{-1}). Therefore, a molecular outflow is undoubtedly associated with the HH 135/136 complex. Fig. 4 presents the map of the blueshifted and redshifted wing emission in the LSR velocity intervals of -29 to -21 km s^{-1} and -15 to -7 km s^{-1}, respectively. This figure shows no clear bipolarity. However, a closer inspection of it reveals a slight displacement between the blueshifted wing component (toward the southwest) and the redshifted wing component (toward the northeast).

4. Discussion

The fact that the redshifted and blueshifted CO wing emission overlaps spatially and shows only a slight indication of bipolarity suggests that the molecular outflow has a wide opening angle. In such a case, even if the line of sight crosses only one cone, the front side of the "red" cone can be blueshifted and the rear side of the "blue" cone redshifted, at least partly explaining the overlap of the blueshifted and redshifted wing emission. Large opening angles of molecular outflows usually indicate that the outflow system has already passed its youngest evolutionary phase (e.g., Shu et al. 1987).

IRAS 11101-5829 has a very high far IR luminosity (1.4 $\times$ 10^4 L$_\odot$, OW92) and could thus be a Herbig Ae/Be star, as suggested by Tamura et al. (1997). HH exciting sources of higher luminosity tend to have higher outflow velocities (Edwards et al. 1991). However, HH 135 and HH 136 do not show high radial velocities for the very high luminosity of the exciting source (OW92). This suggests that the angle between the flow direction and the plane of the sky is small (see below for a quantitative discussion). So we actually have only one cone of the outflow on the line of sight. Cabrit & Bertout (1986) made model calculations of CO line emission from molecular outflows which have various view angles. Fig. 4 is much different from their integrated intensity maps for the case of small angle of the outflow axis from the plane of the sky (see their Fig. 6), which show two separate regions with the blueshifted and redshifted components overlapped. This difference is most probably due to the large beam size, as shown in Fig. 4, compared to the extent of the molecular outflow.

The optical data of HH 135/136 (see Figs. 4a, 4b and 7 of OW92) show that the region just northeast of IRAS 11101-5829 (i.e., the southwestern part of HH 136), has an essentially positive radial velocity, whereas the southwestern side of the IRAS source (i.e., HH 135) has a negative radial velocity. These facts indicate that the high velocity outflow from IRAS 11101-5829 is inclined with respect to the plane of the sky in such a way that the southwestern lobe is approaching us and the northeastern lobe is receding. To the northeast of the source there is the dense cloud core (see Fig. 2). In view of the fact that HH 135 and HH 136 are not heavily reddened (A$_v$=3.1 and 2.8 mag, respectively, out of which the foreground extinction accounts for A$_v$=1.3 mag, see OW92), they are very likely located on the near side of the cloud core. Therefore the receding flow must collide with the core. This collision will deflect the optical outflow and thus can give rise to the velocity shift from the positive to negative values as the flow moves downstream from the southwest to the northeast along the axis of HH 136. This picture can also explain the fact that knots A to C of HH 136 appear to be slightly off (about 7°) the line connecting HH 135, IRAS 11101-5829 and the southwestern part of HH 136 (see also OW92).

The point of impact is probably located near HH 136 knots F and G, where the radial velocity of Hα changes from positive

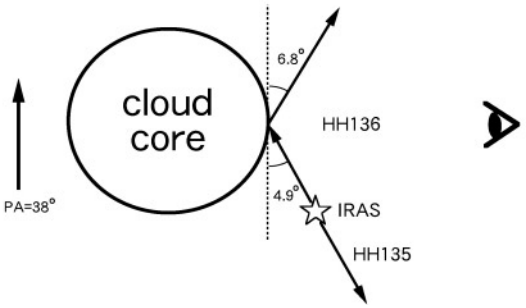

Fig. 5. Configuration of the cloud core, the HH 135/136 outflow and IRAS 11101-5829 as viewed perpendicular to the plane in which they lie.

to negative values (OW92). The cloud core must suffer a strong impact as the outflow rams on it. Do we see any signs of this disturbance? It is interesting to note that a study of the ^{12}CO line profiles (see also Fig. 3) reveals that the position (0″, +15″), which is close to knots F and G, shows a peak $T_A{}^*$(^{12}CO) value of 18 K (cf., e.g., 15 K at the IRAS position). This may be the temperature enhancement reflecting the heating caused by the jet impact. A similar effect has been reported in the interface between the L1642 molecular outflow and the cloud core (Liljeström et al. 1989). We here note that the binary scenario to explain the complicated velocity structure of the HH 135/136 complex is not viable on account of the above-mentioned three facts, namely, the velocity inversion, the slight deflection and the possible temperature enhancement at the midpoint of HH 136.

In two other outflow systems a collisional deflection of the YSO jet has been reported, i.e., HH 110/HH 270 (Reipurth et al. 1996; Olberg 1997) and NGC 2264G (Fich & Lada 1997). Generally the HH 135/136 complex looks somewhat similar to HH 110/HH 270. Reipurth et al. (1996) proposed that the HH 270 jet is deflected by a grazing collision with a dense molecular cloud core and re-emerges as HH 110. In their model both the incident and deflected jets are oriented nearly in the plane of the sky. Thus the true deflection angle is almost equal to the angle defined by the proper motion vectors of HH 110 and HH 270, which is $58°$. In the case of HH 135/136 the above-mentioned small misalignment of the knots suggests that the collision and deflection takes place in a plane roughly perpendicular to the plane of the sky. Thus, the most likely situation can be outlined as in Fig. 5, which is a sketch as viewed perpendicular to the plane where the outflow system, the cloud core center and the observer lie.

Hartigan et al. (1987) showed that in a bow shock the full width at zero intensity (FWZI) of an emission line simply equals to the shock velocity. If we consider only lines that are sufficiently strong and probably unaffected by other emission components (see Fig. 5 of OW92), the mean of the FWZIs of Hα and [NII]6584 in HH 135, of Hα in HH 136A and of [NII]6584 in HH 136B yields a bow shock velocity of 413 ± 21 km s^{-1}. Most probably this is a lower limit, since it is difficult to measure precisely the velocities at zero intensity. Although there are an increasing number of HH objects whose bow shock is known to be traveling through the wake of a previously ejected flow (Ogura 1995; Devine et al. 1997; Eislöffel & Mundt 1997; Reipurth et al. 1997), we assume in the following that the shock velocity is representative also of the optical outflow velocity. The Hα radial velocity of HH 135 with respect to the systemic velocity (-19 km s^{-1}) is -36 km s^{-1} (obtained from the weighted mean of the three Gaussian components, see OW92). Thus the angle between the original flow axis and the plane of the sky is estimated to be $4.9°$. The receding flow then collides with the cloud core and is deflected to suffer an inversion of its radial velocity. The radial velocity of [NII]6584 of HH 136B with respect to the systemic velocity is -49 km s^{-1} (the Hα peak also corresponds to the same value). Combined with the adopted flow velocity of 413 km s^{-1}, this gives an angle of $6.8°$ between the deflected flow direction and the plane of the sky. These small inclination angles are consistent with the line profiles of HH 135 and HH 136B; if we compare them with the line profiles of HH 1/2, HH 32 and Cepheus A given in Hartigan et al. (1987, Figs. 4 to 6), they resemble those of HH 1/2, whose flow axis lies nearly in the plane of the sky, and are much different from those of HH 32 and Cepheus A, which both flow with a large inclination angle. Our first order estimate of the deflection angle is thus about $12°$. In order to obtain more reliable estimates of the optical flow direction and the deflection angle, accurate proper motion data of HH 135 and HH 136 are needed.

5. Conclusions

CO (J=2-1) and ^{13}CO (J=2-1) molecular line observations of the HH 135/136 complex have been presented. The data enabled us to investigate the cloud core and the molecular outflow associated with the optical outflow. The mass of the cloud core is estimated to be some 150 $M_\odot$. The density peak of the cloud is displaced from the power source of the outflow. Presumably this results from the converging shock associated with the curved ionization front (bright rim).

The CO (J=2-1) emission shows high-velocity wings in the vicinity of the power source IRAS 11101-5829. However, the map of the integrated CO wing emission gives only a slight indication of bipolarity. This is most probably due both to a wide opening angle of the molecular outflow and to the large beam size compared to its extent. Since the source is most likely located on the near side of the cloud, the receding lobe collides with the core and is deflected. This explains the velocity inversion observed optically and the slight misalignment of HH knots in the northeastern lobe. From the Hα and [NII] line profiles of the HH knots we derive a deflection angle of about $12°$. The CO (J=2-1) position-velocity diagram and line profiles appear to show a temperature enhancement around the suspected point of flow impact on the cloud core.

Acknowledgements. We would like to express our gratitude to the SEST time allocation committee for the allotment of telescope time. We are also thankful to the referee, Dr. M. Olberg, for the helpful comments. T.L. thanks the Academy of Finland for a travel grant to SEST.

References

Blake G.A., Sutton E.C., Masson C.R., Phillips T.G., 1987, ApJ 315, 621
Booth R.S., Delgado G., Hagstrom M. et al., 1989, A&A 216, 315
Cabrit S., Bertout C., 1986, ApJ 307, 313
Devine D., Bally J., Reipurth B., Heathcote S., 1997, AJ 114, 2095
Dickman R.L., 1978, ApJS 37, 407
Edwards S., Ray T., Mundt R., 1991. In: Levy, E.H., Lunine J.I. (eds.) Protostars and Planets III, University of Arizona Press, p. 567
Eislöffel J., Mundt R., 1997, AJ 114, 280
Eislöffel J., Mundt R., Böhm K.-H., 1994, AJ 108, 1042
Fich M., Lada C.J., 1997, ApJ 484, L63
Gredel R., Reipurth B., 1993, ApJ 407, L29
Hartigan P., Raymond J., Hartmann L., 1987, ApJ 316, 323
Kutner M.L., Ulich, B.L., 1981, ApJ 250, 341
Lefloch B., Lazareff B., 1994, A&A 289, 559
Liljeström T., Mattila K., Friberg, P., 1989, A&A 210, 337
Ogura K., 1995, ApJ 450, L23
Ogura K., Walsh J.R., 1992, ApJ 400, 248 (OW92)
Olberg M. 1997. In: Malbet F., Castets A. (eds.) Poster Proc. IAU Symp. 182, Low Mass Star Formation - from Infall to Outflow, Observatoire de Grenoble, p. 169
Olberg M., Reipurth B., Booth R.S., 1992, A&A 259, 252
Reipurth B., Heathcote S., Roth M. et al., 1993, ApJ 408, L49
Reipurth B., Raga A., Heathcote S., 1996, A&A 311 989
Reipurth B., Bally J., Devine D., 1997, AJ, 114 2708
Shu F.H., Adams F.C., Lizano, S., 1987, ARA&A 25, 23
Stapelfeldt K.R., Scoville N.Z., 1993, ApJ 408, 239
Sugitani K., Ogura K., 1994, ApJS 92, 163
Tamura M., Hough J.H., Chrysostomou A. et al., 1997, MNRAS 287, 894
Ulich B.L., Haas R.W., 1976, ApJS 30, 247